L.M. Vykhor, *DSc (Phys-Math)* [1]
P.V. Gorskyi, *DSc (Phys-Math)* [1,2]
V.V. Lysko, *Cand.Sc (Phys-Math)* [1,2]

[1]Institute of Thermoelectricity of the NAS and MES of Ukraine,
1, Nauky str., Chernivtsi, 58029, Ukraine;
[2]Yuriy Fedkovych Chernivtsi National University,
2, Kotsiubynsky str., Chernivtsi, 58012, Ukraine
e-mail: anatych@gmail.com

METHODS FOR MEASURING CONTACT RESISTANCES OF "METAL – THERMOELECTRIC MATERIAL" STRUCTURES (PART 2)

An overview of existing methods for measuring thermal contact resistance, as well as methods that allow simultaneous determination of thermal and electrical contact resistance values, is presented. Their accuracy, advantages and disadvantages are analyzed, as well as the possibilities of using them in thermoelectricity for the study and optimization of metal-thermoelectric material structures. Bibl. 16, Figs .8.

Key words: thermal contact resistance, electrical contact resistance, measurement, accuracy, thermoelectric power converters.

Introduction

One of the main obstacles to the widespread practical use of thermoelectricity is the high cost of thermoelectric power converters, the largest share of which is the cost of thermoelectric material. Attempts to create miniature modules, and thus significantly reduce their cost, encounter the growing influence of contact resistances, which cause a catastrophic decrease in the quality of the modules.

The development and optimization of technologies for creating contact resistances necessary to meet practical needs is carried out experimentally by studying the influence of various technological factors on the value of contact resistance. The latter is possible only if reliable methods and equipment for measuring contact resistances are available.

The first part of this work present ed an analysis of existing methods and equipment for determining the values of electrical contact resistances and the possibilities of their use for the study and optimization of "metal – thermoelectric material" structures. No less important are the methods for measuring thermal contact resistance, the analysis of which is the subject of the continuation of this work.

1. Specific features of methods for measuring thermal contact resistance

There are a number of methods for measuring thermal contact resistance and the appropriate setups for their implementation. Standard methods are based on measuring the steady heat flux passing through the sample in a specific direction. The basics of the method are set out in the international standard ASTM D5470-06 [1].

In [2], a standard method is described, which is based on the use of a "reference" specimen with a previously known thermal conductivity as a heat flux meter. The diagram of the measuring setup is shown in Fig. 1.

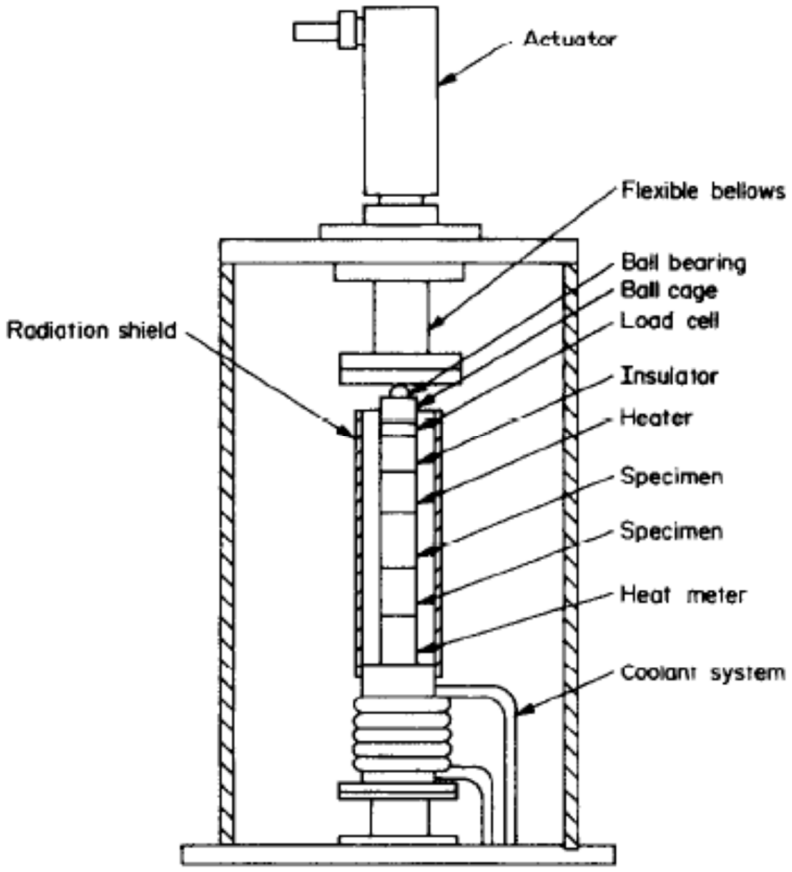

Fig.1. Diagram of a setup for measuring thermal contact resistance using reference specimens as heat meters [2].

The contacting samples are placed between the heater and the heat flux meter. The heat flux is determined by calculation from the known temperature difference and thermal conductivity based on Fourier's law. The calculated power is equal to the heater power. The temperature is measured by three thermocouples mounted in the heat meter at certain distances from the axis. To measure the temperature distribution in the specimens, 36 thermocouples with a diameter of 0.13 mm and a length of 76 cm were used. Thermocouples were placed in holes drilled perpendicular to the specimen axis and fixed in them with epoxy resin. The small diameter of the thermocouples was taken in order to prevent significant disturbance of the heat flux and to fix the position of the thermocouples as accurately as possible. An epoxy resin with a relatively high thermal conductivity was taken so that there was no significant temperature gradient in the bonding layers. The thermocouples partially "wrapped" the heat meter or specimen, which ensured the use of a small piece of the so-called "Kapton tape". Kapton tape has a very low thermal conductivity. Therefore, using this tape to relax the stresses in the thermocouples does not affect the temperature distribution in the specimen or heat meter. Heat losses in such a setup are no more than 2%.

According to [3], some contacts are characterized by the so-called "directional effect", which consists in the fact that the contact resistances measured in two opposite directions to the contact plane differ from each other. One of the hypotheses involved in explaining this phenomenon is the change in the contact geometry depending on the direction of heat propagation due to different mechanical properties of the materials. In most cases, this effect is indeed observed in the contact between dissimilar

materials. However, it can also be observed in the contact between identical materials. Another explanation is that the potential barrier created by oxide layers near the interface weakens the heat transfer by free charge carriers, such as electrons. Let us assume that ε_1 and ε_2 – are the work functions of electrons from metals 1 and 2. Then, if $\varepsilon_1 > \varepsilon_2$, electrons can pass from metal 2 to metal 1, since electrons in the conduction band of metal 2 are energetically closer to the top of the potential barrier. The ratio of conductivities in opposite directions is then equal to:

$$\frac{\sigma_{12}}{\sigma_{21}} = \frac{\tau_{12}}{\tau_{21}} \frac{T_1^2}{T_2^2} \exp\left\{\left(\frac{\varepsilon_1 - \varepsilon_0}{k}\right)\left(\frac{1}{T_2} - \frac{1}{T_1}\right)\right\}. \quad (1)$$

In this formula, ε_0 – is the electron work function from the oxide film. If $\tau_{12} \approx \tau_{21}, \varepsilon_1 > \varepsilon_0, T_1 > T_2$ then $\sigma_{12} > \sigma_{21}$. Work functions are sensitive to the state and preparation of the surface, so there is no reason for the absence of a "directional effect" even in contact between identical materials, if the "histories" of the contacting surfaces are different.

The setup for measuring thermal resistance is shown in Fig.2.

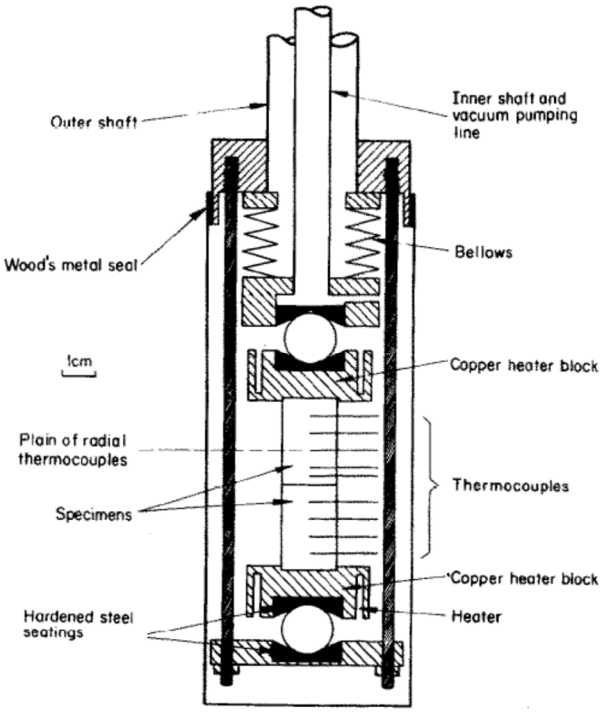

Fig. 2. Schematic diagram of a setup for measuring thermal resistance [3].

The setup is designed to measure contact resistance as a function of load. A load of up to 100 kg is applied kinetically to the contacting specimens, and a heat flux of up to 3 W is "pumped" through them. The heater is powered by a stabilized DC source. The temperature distribution in the specimens is measured by a series of radially placed copper-constantan thermocouples. ThermoEMF is measured with an accuracy of up to 10^{-7} V. The specimens themselves are used as "heat meters". The heat flux through them is calculated from the Fourier law, based on the measured temperature distribution. Under these conditions, the thermal conductivity of the specimens in the temperature range under study is known with sufficient accuracy. The temperature near the interface for each of the contacting specimens, and therefore the temperature jump at the contact, is found by extrapolating the measured temperature

distributions along the length of each of the contacting specimens. The design of the setup ensures a minimal radial temperature gradient. This allows measurements to be made even when the contact resistance is strongly dependent on temperature.

The dimensions of the specimens and the location of the thermocouple holes in them are measured with an accuracy of 1 μm by an optical comparator. After switching on the heater (or cooling in the case of measurements at low temperatures), the contacting specimens were kept until a steady state was reached. At room temperature, a steady state was reached 4-5 hours after a change in the load and approximately 10-12 hours after a change in the direction of the heat flux. In the case of measurements at low temperatures, the indicated terms for reaching the steady state were reduced by approximately half. Smoothing of the experimentally obtained dependences was performed by the least squares method. Pairs of contacting specimens of stainless steel and aluminium were studied in the temperature range of 90-300 K. The dependences of thermal contact resistance on time, load, temperature, magnitude and direction of heat flux were measured. It turned out that the "directional effect" is levelled out as the heat flux increases. At the same time, the value of the inverse specific thermal contact resistance itself depends relatively weakly on the value of the heat flux. Thus, even with a sevenfold increase in the value of the heat flux, the specific thermal contact resistance changes by no more than 10%. Therefore, the specific thermal contact resistance is considered invariant with respect to the value of the heat flux.

In [4], specimens of materials pressed against each other, the contact resistance between which must be measured, are placed in a heat-insulated volume between a heater and a cooler, after which the heat flux through the specimens and the temperatures on both sides of the contact in the immediate vicinity of it are measured (Fig. 3).

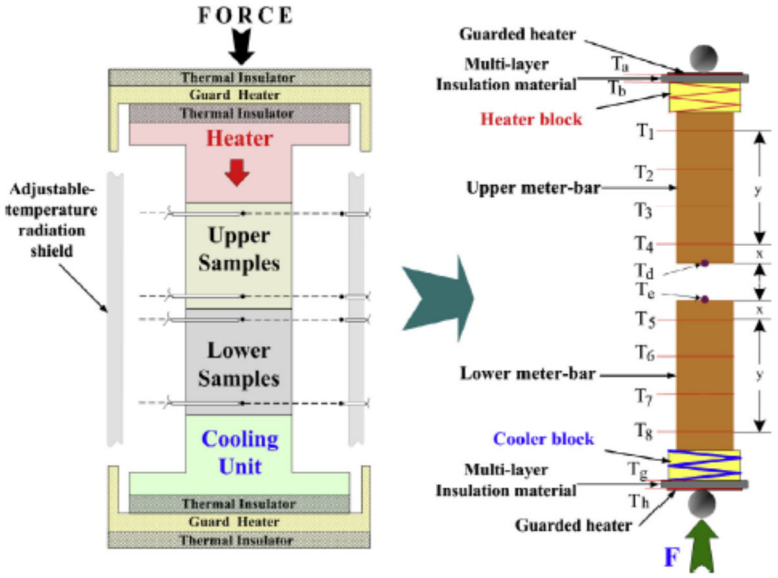

Fig. 3. Schematic diagram of a standard method for measuring contact thermal resistance [4].

A one-dimensional heat flux flows from the upper to the lower specimen and the temperature is distributed linearly, and a jump occurs at the contact. Therefore, the thermal contact resistance is defined as:

$$R = \frac{T_d - T_e}{Q}, \tag{2}$$

where Q is the average heat flux through the contacting specimens. In this case, the temperatures T_d and T_e are determined by extrapolating the temperatures recorded by local sensors placed in the contacting specimens near the interface, to this very interface.

However, the authors of [4] believe that such a standard method gives too large an error and propose a measurement method based on changing the direction of the heat flux. The method is schematically shown in Fig. 4. This method is based on the use of the average value of the thermal contact resistances in the two directions of the heat flux and the symmetry properties of the measuring system. Let the extrapolated temperatures on both sides in the "forward" direction of the heat flux be equal to T_d' and T_e', and in the reverse direction – to T_d'' and T_e''. Then the thermal contact resistance is equal to:

$$R_T = \left[0.5Q\left(\left|T_d' - T_e'\right|^{-1} + \left|T_d'' - T_e''\right|^{-1}\right)\right]^{-1}. \tag{3}$$

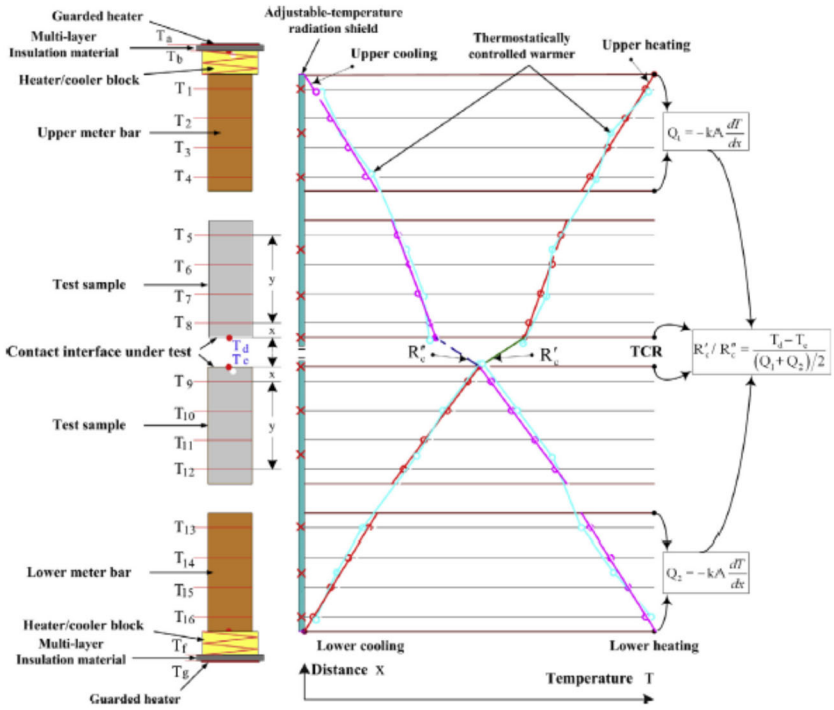

Fig. 4. Schematic diagram for implementation of the variable heat flux method [4].

In [4], it was proven that this method sharply reduces the error, as a result of which the contact resistance ceases to depend on the applied heat flux, while when using the standard method in many cases there is a strong dependence of the results of measuring the thermal contact resistance on the applied heat flux. The temperature in this method is measured by a thermistor.

In general, methods related to measuring thermal characteristics in a steady state are used to measure thermal contact resistance. The disadvantage of these methods is the long waiting time to reach a steady state. In contrast, a number of dynamic methods have been proposed, such as the infrared thermography method [5], the flash method [6], the thermal reflection method [7], the photothermal method [8], and others. [9,10].

As an example, let us consider a non-contact thermographic method described in more detail in [5], which is called the infrared thermography method [5]. According to this method, two contacting

specimens are separately heated to different initial temperatures. Immediately after the specimens reach these temperatures, they are brought into contact. The temperature changes and the heat flux from the hot specimen to the cold one are monitored by a high-speed infrared (IR) camera. This camera records IR radiation in the wavelength range from 7.7 to 9.5 μm. This bandwidth is suitable for measuring temperatures above 20°C. To prevent the influence of ambient radiation, the specimens have a high emissivity or blackness ($\varepsilon = 0.95$), which is achieved by a thin layer of black paint with which the samples are coated. To minimize errors, it is important to determine the temperature near the contact line. For this purpose, an optical system with a resolution of 13 μm/px was used, which is the diffraction limit for the specified wavelength range. With a frame size of 60×80 px, i.e. 780×1040 μm, the frame rate was 2500 Hz. The result of these experiments was the time dependence of the temperature distribution near the contact.

The heat transfer coefficient near the contact cannot be measured directly. It must be determined by solving the inverse problem using information about the temperature at a certain point in the spatial domain. Thus, the "cause" (heat flux) is calculated based on the "effect" (temperature field). The mathematical procedure leads to a single, but unstable solution. Therefore, a small "noise" in the temperature measurement results leads to significant errors in the value of the heat flux.

In the case of a one-dimensional problem, the corresponding partial differential equation with the initial and boundary conditions is given by:

$$\frac{\partial T}{\partial t} = \alpha_T \frac{\partial^2 T}{\partial x^2}, \quad T(x, t=0) = T_0, \quad q_c = -k \frac{\partial T}{\partial x}|_{x=0}, \quad \frac{\partial T}{\partial x}|_{x\to\infty}, \tag{4}$$

where α_T is thermal diffusivity. Then the desired heat transfer coefficient is determined as:

$$h_c = \frac{q_c}{\Delta T}. \tag{5}$$

Although the contacting bodies are bounded, the contact time is too short for the heat flux to reach the distant boundaries of the bodies, so the bodies can be considered semi-bounded.

To calculate the heat transfer coefficient, it is necessary to determine the heat flux through the contact area. It is determined using a step-by-step procedure involving a number of "future points in time." The algorithm for calculating the heat flux is illustrated by the following equation:

$$q_c(x=0, t_m) = \frac{\sum_{i=1}^{r} \left(T_{\text{meas},m+i-1} - T_{m+i-1}\right) \Phi_i(x = x_1, t_i)}{\sum_{i=1}^{r} \Phi_i^2(x = x_1, t_i)}, \tag{6}$$

where the step corresponds to a unit jump in the heat flux for a semi-bounded body, which is defined as

$$\Phi_i(x,t) = \frac{x}{k}\sqrt{\frac{4\alpha_T t}{\pi}}\left[\frac{1}{\sqrt{\pi}}\exp\left(-\frac{1}{\sqrt{Fo}}\right) - \frac{1}{2\sqrt{Fo}}\operatorname{erfc}\left(\frac{1}{2\sqrt{Fo}}\right)\right], \tag{7}$$

where $F_0 = \alpha_T t / x^2$ is the Fourier number. Eq. (7) contains only the physical constants of the material and the coordinate and time. Therefore, the corresponding calculation is performed once, namely at the beginning of the procedure. Eq. (6) is obtained from considerations of minimizing the root mean square deviation between the measured ($T_{\text{meas},m}$) and calculated (T_m) temperatures.

Thus, the final contact resistance is calculated based on the measured temperature distribution

and the calculated heat flux. The temperature difference is measured not directly at the contact, but at a distance of 50-100 microns from it, since otherwise the data is too "noisy" due to the deformation of the bodies. Under these conditions, the difference between the true temperature jump and the measurement data is neglected. The schematic diagram for determining the heat flux through the contact by the superposition method is shown in Fig. 5. The true heat transfer coefficient is considered to be its steady-state value over time. The sought thermal contact resistance is equal to the inverse heat transfer coefficient.

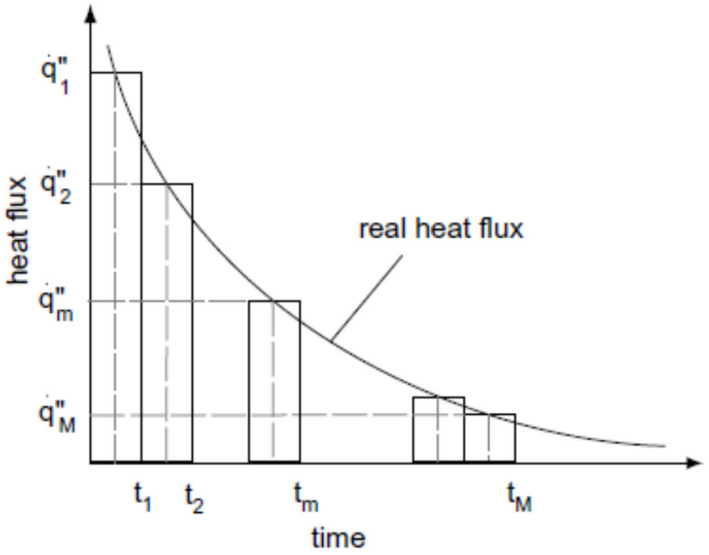

Fig. 5. Schematic diagram for determining the heat flux through the contact by the superposition method [5].

In [11], a method for measuring the thermal resistance between a conductive film and a substrate was proposed, which is suitable for measuring the thermal resistance of contacts created in thermoelectric products in a "microelectronic" design, when a metal contact layer is sprayed or deposited on a thin semiconductor layer. The schematic diagram of the measuring setup for implementing this method is shown in Fig. 6.

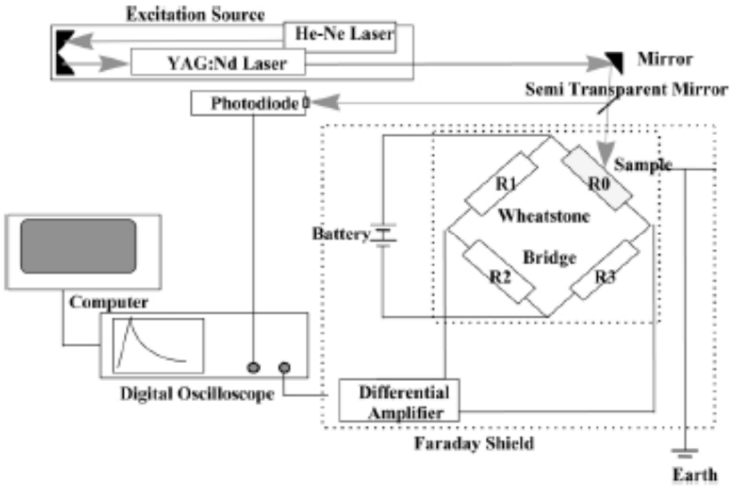

Fig. 6. Schematic diagram for measuring the thermal resistance of a specimen in the form of a thin film on a substrate [11].

In this diagram, the specimen (film on the substrate) was heated by laser pulses with an energy of 4 J and a duration of 20 ns from a neodymium laser with a wavelength of radiation of 1.06 μm. The neodymium laser was pumped by a helium-neon laser. In order to measure the temperature, the specimen was connected to a Wheatstone bridge. A constant voltage was applied to one of the diagonals of the bridge. The voltage removed from the other diagonal of the bridge, as a result of heating and subsequent cooling of the specimen, depended on time. This voltage was fed through a differential amplifier to the input of a digital oscilloscope. The Wheatstone bridge together with the differential amplifier was placed in a Faraday cage. The second input was supplied with a reference voltage from a photodiode, which was illuminated by the same laser that heated the specimen through a semi-transparent mirror. The computer processed the time dependence of this voltage after the peak, since it was it that characterized the cooling of the specimen. Thermal resistance is determined simultaneously with thermal conductivity by fitting experimental thermograms to theoretical ones in the time interval from 10^{-7} to 10^{-6} s. Thermal contact resistance is calculated by the least squares method.

2. Methods for simultaneous measurement of thermal and electrical contact resistances

Methods for simultaneous measurement of thermal R_t and electrical R_c contact resistances are described in [12-14].

In [12], methods for measuring the temperature dependences of thermal and electrical contact resistances are presented. The methods were developed to study the properties of the boundary layer between the thermoelectric oxide material of p-type conductivity $Ca_3Co_4O_3$and the Fe-Cr alloy, which can be used as a material for a connecting plate in the manufacture of generator thermoelectric modules from oxide-based materials. The studied two-layer samples of Fe-Cr/ $Ca_3Co_4O_3$ were obtained using SPS sintering technology. In [13], similar methods were used to study the thermal and electrical contact resistances of two-layer specimens of Ni/ $Ca_3Co_4O_3$.

The thermal contact resistance R_t was determined by measuring the thermal diffusivity by the laser flash method using a special device "Netzch LFA-457 Laser Flash Apparatus". Initially, the thermal diffusivity of each of the Fe-Cr and $Ca_3Co_4O_3$ materials is determined separately. Then measurements are made on two-layer washers. Thin washers (1–2 mm) are used for this. The time t_i is measured during which a strong energy pulse created on the surface of the washer causes half the maximum temperature deviation on the opposite surface of the washer. Thermal diffusivity α is calculated using a simple formula [15]

$$\alpha_i = 1.37a^2 / \pi^2 t_i , \tag{8}$$

where a is washer thickness. Corrections to formula (12) for a more accurate method of calculating thermal diffusivity are described in [16].

The measurement data for single and double-layer washers are automatically used as input data for special computer programs which the Netzch LFA-457 installation is equipped with. This software is designed and configured to determine the thermal contact resistance of the double-layer model.

The electrical contact resistance was measured in the temperature range from 30°C to 800°C on two-layer column-shaped specimens. The measurement diagram is shown in Fig. 7 [12].

This model allows measuring both the resistivity of each specimen component and the contact resistance 4 of the boundary, which is determined by linear extrapolation of the dependence of the resistance R on the distance x to the boundary ($x_{n\,\text{to}\,0}$) by the formula

$$R_c = \text{extrapolation}\,(R\ \ from\ x_{6-3\ to\ 0}) - R_{1-2}\frac{x_{1-2}}{x_{2-0}} \tag{9}$$

The last term in formula (9) accounts for the contribution from the influence of the resistance of the *Fe-Cr* alloy between the probe and the boundary.

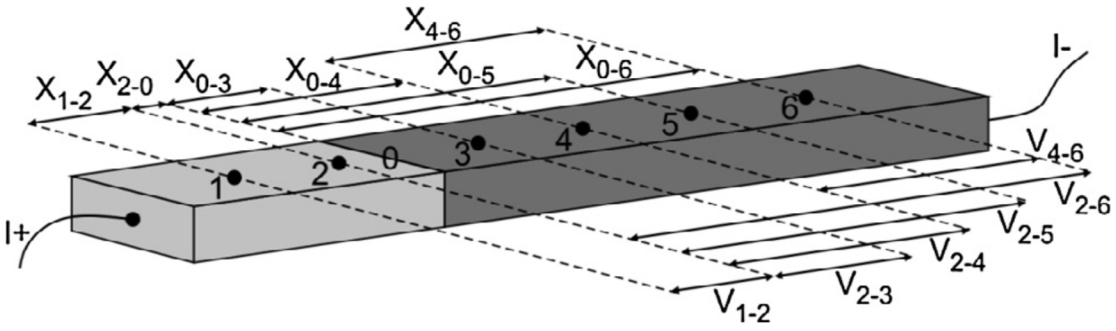

Fig. 7. Schematic diagram for measuring electrical contact resistance [12].

The voltage at different points is measured with a 4-probe Keithley Micro-ohmmeter. The distance from the probes to the boundary is measured using an Olympus SZX9 Stereomicroscope.

Using a micro-ohmmeter, a current was applied to the specimen and the voltage was measured at various points along the surface of the specimen using a probe made of platinum wire with a diameter of 0.1 mm, which was attached with silver paste. The micro-ohmmeter was operated in pulse mode with current passing and voltage measurement for 150 ms. The current was then switched off and the voltage caused by the temperature gradient (due to thermoEMF) was measured and taken into account in determining the resistance. Measurements were made for the forward and reverse directions of the current and the results were averaged. The values of the thermal and electrical resistance of the boundary were multiplied by the cross-sectional area of the measured samples, which gave the value of the specific contact resistance.

[14] describes a setup designed to measure both electrical and thermal contact resistance. Simultaneous measurement of R_c and R_t of a junction is important for understanding the relationship between the quantities and their possible influence on each other. Such data can be useful for designing improved electrical and thermal contacts between materials.

The electrical contact resistance R_c is measured using the 4-probe method (Kelvin method) on direct current. To measure the thermal contact resistance R_t, the heat flux power Q through the contact boundary in steady state is determined using data on a material with known thermal conductivity and the temperature gradient in the unit under study, and ΔT at the boundary is calculated from measurements and extrapolation of the temperature gradient in the specimens. The thermal conductivity of the contact is determined by the formula

$$h_t = \frac{Q}{A\Delta T}, \tag{10}$$

where A is contact area.

The measurement chamber contains two heater-cooler units, two heat flux meters and two test specimens that are joined together, as shown in Fig. 8a. The units and meters are placed symmetrically to the contact boundary of the specimens. The chamber can be evacuated to 10^{-6} mbar or filled with gas. Measurements can be carried out at temperatures from 20 to 150°C. Constant temperatures are created

by the heater and the cooling system. The contact of the two specimens is formed by compression using a hydraulic system. The pressure can vary from 0 to 500 kg. Cylindrical samples with a diameter of 10 to 30 mm and a height of 20 to 100 mm can be used for research. The specimen under study is connected to electrical and thermal sensors, as shown in Fig. 8b.

The heater-cooler units are made in the form of copper cylinders. The copper tubes of the cooler are placed in the grooves in the form of a spiral. The nichrome heating elements, inserted into the ceramic washers, are fastened with clamps. The unit can operate as a heater when voltage is supplied to the heating elements, or as a cooler when a coolant is supplied to the copper tubes. In this way, the direction of the heat flux can be changed without disturbing any processes.

Heat flux meters are also cylindrical units made of copper with a known thermal conductivity. The amount of heat flowing through the meter is calculated by measuring the temperature gradients in the direction of the heat flux. The error in determining heat flux using these meters is ±5%.

A digital multimeter (DMM), which measures electrical resistance to an accuracy of 0.1 μΩ, is used to determine electrical contact resistance. The DMM is set up for 4-probe measurements under conditions of minimizing the contribution of wire resistance, including solder joints. The DMM is connected to a computer with special measurement software. The electrical circuit for thermal measurements is completely separated from the electrical circuit, including the DMM and the computer.

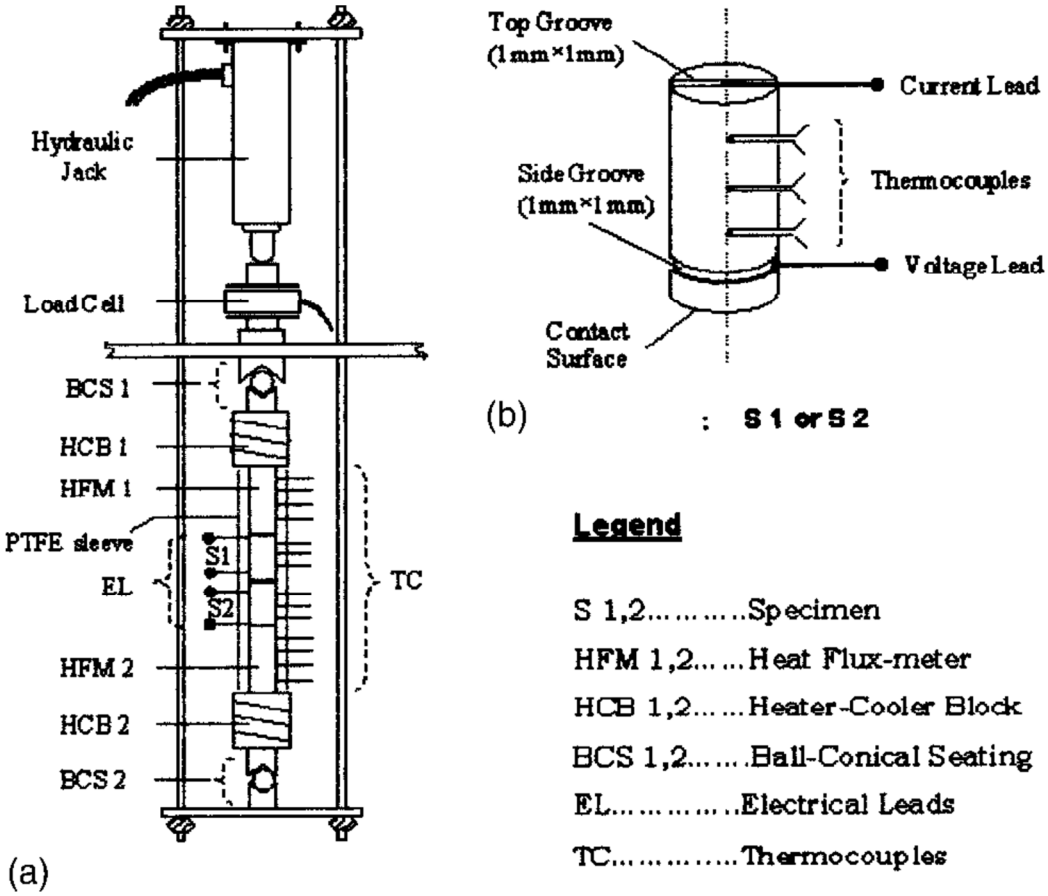

Fig. 8. Schematic of a chamber for measuring contact resistances [14].

In [14], an example of the results of measuring the electrical and thermal contact resistances for a brass/brass pressure contact is presented. It was found that the absolute maximum deviation when measuring the electrical contact resistance on the described setup is ±0.003%, and the thermal

conductivity of the contact is ±4.4%. The setup can also be used for measuring the thermal conductivity of materials.

Conclusions

1. The examination and analysis of existing methods for measuring thermal contact resistance, as well as methods that allow the simultaneous determination of thermal and electrical contact resistance values, highlights both the advantages and disadvantages of individual methods.
2. The accuracy and reliability of methods for measuring contact thermal resistance, as well as methods for measuring electrical contact resistance, require significant improvement to implement in practice the possibilities for reducing contact resistances provided by theoretical studies.

References

1. *ASTM 2009*, Standard test method for thermal conductivity of solids by means of the guarded-comparative-longitudinal heat flow technique E1225 – 09.
2. McWaid T., Marshall E. (1992). Thermal contact resistance across pressed metal contacts in a vacuum environment. *Int. J. Heat and Mass Transfer*, 35 (11), 2911 – 2920.
3. Thomas T.R., Probert S.D. (1970). Thermal contact resistance: directional effect and other problems. *Int. J. Heat and Mass Transfer*, 13, 789 – 807.
4. Ping Zhang, Yi Min Xuan, Qiang Li. (2014). A high-precision instrumentation of measuring thermal contact resistance using reversible heat flux. *Experimental Thermal and Fluid Science,* 54, 204 – 211.
5. Fieberg C., Kneer R. (2008). Determination of thermal contact resistance from transient temperature measurement. *Int. J. Heat and Mass Transfer*, 51, 1017 – 1023.
6. N.D. Miloševicr. (2008). Determination of transient thermal interface resistance between two bonded metal bodies using the Laser-Flash method. *Int. J. Thermophys*., 29, 2072 – 2087.
7. Smith A.N., Hosteler J.L. (2000). Thermal boundary resistance measurements using a transient thermo-reflectance technique. *Microscale Therm. Eng*., 4, 51 – 60.
8. Shi L., Wang H.L. (2007). Investigation on thermal contact resistance by photothermal technique at low temperature. *Int. J. Heat Mass Tran*., 43 (11), 1179 – 1184.
9. Cong P.Z., Zhang X., Fujii M. (2006). Estimation of thermal contact resistance using ultrasonic waves, *Int. J. Thermophys*., 27, 171 – 183.
10. Lisker I.S., Solovyev S.V. (2001). A transient technique for measuring the thermal conductivity of non-metals. *Exp. Therm. Fluid Sci*., 25, 377 – 382.
11. Lahmar A., Nguen T.P., Sakami D., Orain S., Scudeller U., Danes F. (2001). Experimental investigation on the thermal contact resistance between gold coating and ceramic substrate. *Thin Solid Films*, 389, 167 – 172.
12. Holgate Tomas C., Han Li, Wu Ning Yu, Bojesen Espen D., Christensen Mogens, Iversen Bo B., Nong Ngo Van, Pryds Nini (2014). Characterization of the interface between an *Fe-Cr* alloy and the *p*-type thermoelectric oxide $Ca_3Co_4O_9$. *Journal of Alloys and Compounds*, 582, 827 – 833.
13. Holgate T.C., Wu N., Sondergaard M., Iversen B.B., Nong N.V., Pryds N. (2013). Kinetics, stability, and thermal contact resistance of nickel – $Ca_3Co_4O_9$ interfaces formed by spark plasma sintering. *J. of Electronic Materials*, 42(7), 1661 – 1668.

14. Misra Prashant, Nagarajua J. (2004). Test facility for simultaneous measurement of electrical and thermal contact resistance. *Review of Scientific Instruments*, 75 (8), 2625 – 2630.
15. Parker W.J., Jenkins R.J., Butler C.P. and Abbott G.L. (1961). *J. App. Phys*. 32, 1679.
16. Cape J.A., Lehman G.W. (1963). Temperature and finite pulse-time effects in the flash method for measuring thermal diffusivity. *J. of Applied Physics*, 34 (7), 1909 – 1913.

Submitted 23.08.2022.

Вихор Л.М., *доктор фіз.-мат. наук* [1]
Горський П.В., *доктор фіз.-мат. наук* [1,2]
Лисько В.В., *канд. фіз.-мат. наук* [1,2]

[1] Інститут термоелектрики НАН та МОН України,
вул. Науки, 1, Чернівці, 58029, Україна;
[2] Чернівецький національний університет імені Юрія Федьковича,
вул. Коцюбинського 2, Чернівці, 58012, Україна
e-mail: anatych@gmail.com

МЕТОДИ ВИМІРЮВАННЯ КОНТАКТНИХ ОПОРІВ СТРУКТУР «МЕТАЛ – ТЕРМОЕЛЕКТРИЧНИЙ МАТЕРІАЛ» (ЧАСТИНА 2)

Наведено огляд існуючих методів вимірювання теплового контактного опору, а також методів, що дозволяють одночасно визначати величини і теплового, і електричного контактних опорів. Проведено аналіз їх точності, переваг та недоліків, а також можливостей використання у термоелектриці для дослідження та оптимізації структур «метал – термоелектричний матеріал». Бібл. 16, рис .8.

Ключові слова: тепловий контактний опір, електричний контактний опір, вимірювання, точність, термоелектричні перетворювачі енергії.

Література

1. *ASTM 2009*, Standard test method for thermal conductivity of solids by means of the guarded-comparative-longitudinal heat flow technique E1225 – 09.
2. McWaid T., Marshall E. (1992). Thermal contact resistance across pressed metal contacts in a vacuum environment. *Int. J. Heat and Mass Transfer*, 35 (11), 2911 – 2920.
3. Thomas T.R., Probert S.D. (1970). Thermal contact resistance: directional effect and other problems. *Int. J. Heat and Mass Transfer*, 13, 789 – 807.
4. Ping Zhang, Yi Min Xuan, Qiang Li. (2014). A high-precision instrumentation of measuring thermal contact resistance using reversible heat flux. *Experimental Thermal and Fluid Science,* 54, 204 – 211.
5. Fieberg C., Kneer R. (2008). Determination of thermal contact resistance from transient temperature measurement. *Int. J. Heat and Mass Transfer*, 51, 1017 – 1023.
6. N.D. Miloševicґ. (2008). Determination of transient thermal interface resistance between two bonded metal bodies using the Laser-Flash method. *Int. J. Thermophys*., 29, 2072 – 2087.
7. Smith A.N., Hosteler J.L. (2000). Thermal boundary resistance measurements using a transient thermo-reflectance technique. *Microscale Therm. Eng*., 4, 51 – 60.

8. Shi L., Wang H.L. (2007). Investigation on thermal contact resistance by photothermal technique at low temperature. *Int. J. Heat Mass Tran*., 43 (11), 1179 – 1184.
9. Cong P.Z., Zhang X., Fujii M. (2006). Estimation of thermal contact resistance using ultrasonic waves, *Int. J. Thermophys*., 27, 171 – 183.
10. Lisker I.S., Solovyev S.V. (2001). A transient technique for measuring the thermal conductivity of non-metals. *Exp. Therm. Fluid Sci*., 25, 377 – 382.
11. Lahmar A., Nguen T.P., Sakami D., Orain S., Scudeller U., Danes F. (2001). Experimental investigation on the thermal contact resistance between gold coating and ceramic substrate. *Thin Solid Films*, 389, 167 – 172.
12. Holgate Tomas C., Han Li, Wu Ning Yu, Bojesen Espen D., Christensen Mogens, Iversen Bo B., Nong Ngo Van, Pryds Nini (2014). Characterization of the interface between an *Fe-Cr* alloy and the *p*-type thermoelectric oxide $Ca_3Co_4O_9$. *Journal of Alloys and Compounds*, 582, 827 – 833.
13. Holgate T.C., Wu N., Sondergaard M., Iversen B.B., Nong N.V., Pryds N. (2013). Kinetics, stability, and thermal contact resistance of nickel – $Ca_3Co_4O_9$ interfaces formed by spark plasma sintering. *J. of Electronic Materials*, 42(7), 1661 – 1668.
14. Misra Prashant, Nagarajua J. (2004). Test facility for simultaneous measurement of electrical and thermal contact resistance. *Review of Scientific Instruments*, 75(8), 2625 – 2630.
15. Parker W.J., Jenkins R.J., Butler C.P. and Abbott G.L. (1961). *J. App. Phys*. 32, 1679.
16. Cape J.A., Lehman G.W. (1963). Temperature and finite pulse-time effects in the flash method for measuring thermal diffusivity. *J. of Applied Physics*, 34 (7), 1909 – 1913.

Надійшла до редакції: 23.08.2022.